

# Negative Horizon Mass for Rotating Black Holes

**Jutta Kunz** and **Francisco Navarro-Lérida**

Institut für Physik, Universität Oldenburg, Postfach 2503  
D-26111 Oldenburg, Germany

October 11, 2018

## Abstract

Charged rotating black holes of Einstein-Maxwell-Chern-Simons theory in odd dimensions,  $D \geq 5$ , may possess a negative horizon mass, while their total mass is positive. This surprising feature is related to the existence of counterrotating solutions, where the horizon angular velocity  $\Omega$  and the angular momentum  $J$  possess opposite signs. Black holes may further possess vanishing horizon angular velocity while they have finite angular momentum, or they may possess finite horizon angular velocity while their angular momentum vanishes. In  $D = 9$  even non-static black holes with  $\Omega = J = 0$  appear. Charged rotating black holes with vanishing gyromagnetic ratio exist, and black holes need no longer be uniquely characterized by their global charges.

# 1 Introduction

The Kerr-Newman (KN) family of black hole solutions of Einstein-Maxwell (EM) theory [1] possesses many special properties, not present in black hole solutions of theories with more general matter content. The inclusion of a dilaton, for instance, leads to deviations of the gyromagnetic ratio from the KN value [2], and when the dilaton coupling exceeds the Kaluza-Klein value counterrotating black holes appear, where the horizon rotates in the opposite sense to the total angular momentum [3]; while the EM uniqueness theorem or Israel's theorem [4] do not hold in general in theories with non-Abelian fields [5, 6].

In the context of supergravity or string theory, higher dimensional black holes are of interest. The Myers-Perry solutions [7], representing higher dimensional rotating vacuum black holes, have long been known, as well as various charged rotating black holes of supergravity and string theory [8]. In contrast, the higher dimensional generalization of the KN black holes has so far resisted attempts to obtain them in analytical form [9, 10].

In odd dimensions,  $D = 2N + 1$ , the EM action may be supplemented by an ' $A F^N$ ' Chern-Simons (CS) term. In 5 dimensions, for a certain value of the CS coefficient  $\lambda = \lambda_{\text{SG}}$ , the theory corresponds to the bosonic sector of  $D = 5$  supergravity, where rotating black hole solutions are known analytically [11, 12]. In particular, extremal solutions exist, whose horizon angular velocity vanishes. Thus their horizon is non-rotating, although their angular momentum is nonzero. In these solutions a negative fraction of the total angular momentum is stored in the Maxwell field behind the horizon, and the effect of rotation on the horizon is not to make it rotate but to deform it into a squashed 3-sphere [13, 14]. Here supersymmetry is associated with a borderline between stability and instability, since for  $\lambda > \lambda_{\text{SG}}$  a rotational instability arises, where counterrotating black holes appear [15]. Moreover, when the CS coefficient is increased beyond the  $2\lambda_{\text{SG}}$ , black holes (with horizon topology of a sphere [16]) are no longer uniquely characterized by their global charges [15].

Here we reanalyze 5-dimensional Einstein-Maxwell-Chern-Simons (EMCS) black holes and show, that they may possess a negative horizon mass for a CS coefficient beyond  $2\lambda_{\text{SG}}$ . We also investigate their higher dimensional generalizations for arbitrary CS coefficient. While  $D = 2N + 1$ -dimensional black holes generically possess  $N$  independent angular momenta [7], we here focus on black holes with equal-magnitude angular momenta [10], allowing for the reduction of the EMCS equations to a set of ordinary differential equations. In section 2 we recall the EMCS action and present the appropriate Ansätze for the metric and the gauge potential. We discuss the black hole properties in section 3. We present the numerical results for  $D = 5$  and  $D > 5$  black holes in section 4, and summarize in section 5.

## 2 Action, Metric and Gauge Potential

We consider the odd  $D$ -dimensional EMCS action with Lagrangian [13]

$$L = \frac{1}{16\pi G_D} \sqrt{-g} \left( R - F_{\mu\nu} F^{\mu\nu} + \frac{8}{D+1} \tilde{\lambda} \epsilon^{\mu_1 \mu_2 \dots \mu_{D-2} \mu_{D-1} \mu_D} F_{\mu_1 \mu_2} \dots F_{\mu_{D-2} \mu_{D-1}} A_{\mu_D} \right), \quad (1)$$

with curvature scalar  $R$ ,  $D$ -dimensional Newton constant  $G_D$ , and field strength tensor  $F_{\mu\nu} = \partial_\mu A_\nu - \partial_\nu A_\mu$ , where  $A_\mu$  denotes the gauge potential.  $\tilde{\lambda}$  corresponds to the CS coupling constant.

The field equations are obtained from the action Eq. (1) by taking variations with respect to the metric and the gauge potential, yielding the Einstein equations

$$G_{\mu\nu} = R_{\mu\nu} - \frac{1}{2} g_{\mu\nu} R = 2T_{\mu\nu}, \quad (2)$$

with stress-energy tensor

$$T_{\mu\nu} = F_{\mu\rho} F_\nu{}^\rho - \frac{1}{4} g_{\mu\nu} F_{\rho\sigma} F^{\rho\sigma}, \quad (3)$$

and the gauge field equations

$$\nabla_\nu F^{\mu_1 \nu} = \tilde{\lambda} \epsilon^{\mu_1 \mu_2 \mu_3 \dots \mu_{D-1} \mu_D} F_{\mu_2 \mu_3} \dots F_{\mu_{D-1} \mu_D}. \quad (4)$$

In order to obtain stationary black hole solutions of Eqs. (2)-(4), representing charged generalizations of the odd  $D$ -dimensional Myers-Perry solutions [7], we consider black hole space-times with  $N$ -azimuthal symmetries, implying the existence of  $N+1$  commuting Killing vectors,  $\xi \equiv \partial_t$ , and  $\eta_{(k)} \equiv \partial_{\varphi_k}$ , for  $k = 1, \dots, N$ , where  $N$  is defined by  $D = 2N + 1$ .

While generic EMCS black holes possess  $N$  independent angular momenta, we now restrict to black holes whose angular momenta have all equal magnitude. The metric and the gauge field parametrization then simplify considerably. In particular, for such equal-magnitude angular momenta black holes, the general Einstein and gauge field equations reduce to a set of ordinary differential equations [10], since the angular dependence can be treated explicitly.

Restricting to black holes with spherical horizon topology, we parametrize the metric in isotropic coordinates, which are well suited for the numerical construction of rotating black holes [9, 15, 17],

$$ds^2 = -f dt^2 + \frac{m}{f} \left[ dr^2 + r^2 \sum_{i=1}^{N-1} \left( \prod_{j=0}^{i-1} \cos^2 \theta_j \right) d\theta_i^2 \right] + \frac{n}{f} r^2 \sum_{k=1}^N \left( \prod_{l=0}^{k-1} \cos^2 \theta_l \right) \sin^2 \theta_k \left( \varepsilon_k d\varphi_k - \frac{\omega}{r} dt \right)^2$$

$$\begin{aligned}
& + \frac{m-n}{f} r^2 \left\{ \sum_{k=1}^N \left( \prod_{l=0}^{k-1} \cos^2 \theta_l \right) \sin^2 \theta_k d\varphi_k^2 \right. \\
& \left. - \left[ \sum_{k=1}^N \left( \prod_{l=0}^{k-1} \cos^2 \theta_l \right) \sin^2 \theta_k \varepsilon_k d\varphi_k \right]^2 \right\} , \tag{5}
\end{aligned}$$

where  $\theta_0 \equiv 0$ ,  $\theta_i \in [0, \pi/2]$  for  $i = 1, \dots, N-1$ ,  $\theta_N \equiv \pi/2$ ,  $\varphi_k \in [0, 2\pi]$  for  $k = 1, \dots, N$ , and  $\varepsilon_k = \pm 1$  denotes the sense of rotation in the  $k$ -th orthogonal plane of rotation.

The parametrization for the gauge potential, consistent with Eq. (5), is

$$A_\mu dx^\mu = a_0 dt + a_\varphi \sum_{k=1}^N \left( \prod_{l=0}^{k-1} \cos^2 \theta_l \right) \sin^2 \theta_k \varepsilon_k d\varphi_k . \tag{6}$$

It is remarkable that, independent of the odd dimension  $D \geq 5$ , this parametrization involves only four functions  $f, m, n, \omega$  for the metric and two functions  $a_0, a_\varphi$  for the gauge field, which all depend only on the radial coordinate  $r$ .

## 3 Black Hole Properties

### 3.1 Boundary conditions

By substituting Eqs. (5)-(6) in Eqs. (2)-(4), a system of 6 ordinary differential equations is obtained. In order to generate black hole solutions, appropriate boundary conditions have to be imposed.

For asymptotically flat solutions, the metric functions should satisfy at infinity the boundary conditions

$$f|_{r=\infty} = m|_{r=\infty} = n|_{r=\infty} = 1 , \quad \omega|_{r=\infty} = 0 . \tag{7}$$

For the gauge potential we choose a gauge, in which it vanishes at infinity

$$a_0|_{r=\infty} = a_\varphi|_{r=\infty} = 0 . \tag{8}$$

The horizon is located at  $r = r_H$ , and is characterized by the condition  $f(r_H) = 0$  [17]. Requiring the horizon to be regular, the metric functions must satisfy the boundary conditions

$$f|_{r=r_H} = m|_{r=r_H} = n|_{r=r_H} = 0 , \quad \omega|_{r=r_H} = r_H \Omega , \tag{9}$$

where  $\Omega$  is (related to) the horizon angular velocity, defined in terms of the Killing vector

$$\chi = \xi + \Omega \sum_{k=1}^N \varepsilon_k \eta_{(k)} , \tag{10}$$

which is null at the horizon. The gauge potential satisfies

$$\chi^\mu A_\mu|_{r=r_H} = \Phi_H = (a_0 + \Omega a_\varphi)|_{r=r_H} , \quad \left. \frac{da_\varphi}{dr} \right|_{r=r_H} = 0 , \quad (11)$$

with constant horizon electrostatic potential  $\Phi_H$ .

### 3.2 Global charges

Since the space-times we are considering are stationary, (multi-)axisymmetric, and asymptotically flat we may compute the mass  $M$  and the  $N$  angular momenta  $J_{(k)}$  of the black holes by means of the Komar expressions associated with the respective Killing vector fields

$$M = \frac{-1}{16\pi G_D} \frac{D-2}{D-3} \int_{S_\infty^{D-2}} \alpha , \quad J_{(k)} = \frac{1}{16\pi G_D} \int_{S_\infty^{D-2}} \beta_{(k)} , \quad (12)$$

with  $\alpha_{\mu_1 \dots \mu_{D-2}} \equiv \epsilon_{\mu_1 \dots \mu_{D-2} \rho \sigma} \nabla^\rho \xi^\sigma$ ,  $\beta_{(k)\mu_1 \dots \mu_{D-2}} \equiv \epsilon_{\mu_1 \dots \mu_{D-2} \rho \sigma} \nabla^\rho \eta_{(k)}^\sigma$ . For equal-magnitude angular momenta  $J_{(k)} = \varepsilon_k J$ ,  $k = 1, \dots, N$ .

The electric charge  $Q$  associated with the Maxwell field can be defined by

$$Q = \frac{-1}{8\pi G_D} \int_{S_\infty^{D-2}} \tilde{F} , \quad (13)$$

with  $\tilde{F}_{\mu_1 \dots \mu_{D-2}} \equiv \epsilon_{\mu_1 \dots \mu_{D-2} \rho \sigma} F^{\rho \sigma}$ .

These global charges and the magnetic moment  $\mu_{\text{mag}}$  can be obtained from the asymptotic expansions of the metric and the gauge potential

$$f = 1 - \frac{\hat{M}}{r^{D-3}} + \dots , \quad \omega = \frac{\hat{J}}{r^{D-2}} + \dots , \quad a_0 = \frac{\hat{Q}}{r^{D-3}} + \dots , \quad a_\varphi = -\frac{\hat{\mu}_{\text{mag}}}{r^{D-3}} + \dots , \quad (14)$$

where

$$\begin{aligned} \hat{M} &= \frac{16\pi G_D}{(D-2)A(S^{D-2})} M , & \hat{J} &= \frac{8\pi G_D}{A(S^{D-2})} J , \\ \hat{Q} &= \frac{4\pi G_D}{(D-3)A(S^{D-2})} Q , & \hat{\mu}_{\text{mag}} &= \frac{4\pi G_D}{(D-3)A(S^{D-2})} \mu_{\text{mag}} , \end{aligned} \quad (15)$$

and  $A(S^{D-2})$  denotes the area of the unit  $(D-2)$ -sphere. The gyromagnetic ratio  $g$  is then defined via

$$g = 2 \frac{M \mu_{\text{mag}}}{Q J} . \quad (16)$$

### 3.3 Mass formulae

The surface gravity  $\kappa$  of the black holes is defined by

$$\kappa^2 = -\frac{1}{2} \lim_{r \rightarrow r_{\text{H}}} (\nabla_{\mu} \chi_{\nu}) (\nabla^{\mu} \chi^{\nu}) . \quad (17)$$

For equal-magnitude angular momenta, the area of the horizon  $A_{\text{H}}$  reduces to

$$A_{\text{H}} = r_{\text{H}}^{D-2} A(S^{D-2}) \lim_{r \rightarrow r_{\text{H}}} \sqrt{\frac{m^{D-3} n}{f^{D-2}}} . \quad (18)$$

The horizon mass  $M_{\text{H}}$  and horizon angular momenta  $J_{\text{H}(k)}$  are given by

$$M_{\text{H}} = \frac{-1}{16\pi G_D} \frac{D-2}{D-3} \int_{\mathcal{H}} \alpha , \quad J_{\text{H}(k)} = \frac{1}{16\pi G_D} \int_{\mathcal{H}} \beta_{(k)} , \quad (19)$$

where  $\mathcal{H}$  represents the surface of the horizon, and for equal-magnitude angular momenta  $J_{\text{H}(k)} = \varepsilon_k J_{\text{H}}$ ,  $k = 1, \dots, N$ . The mass  $M$  and angular momenta  $J_{(k)}$  may thus be reexpressed in the form [13, 14]

$$M = M_{\text{H}} + M_{\Sigma} , \quad J_{(k)} = J_{\text{H}(k)} + J_{\Sigma(k)} , \quad (20)$$

where  $J_{\Sigma(k)}$  is a ‘bulk’ integral over the region of  $\Sigma$  outside the horizon, i.e.,  $\Sigma$  is a space-like hypersurface with boundaries at spatial infinity and on the horizon.

The black holes satisfy the horizon mass formula

$$\frac{D-3}{D-2} M_{\text{H}} = \frac{\kappa A_{\text{H}}}{8\pi G_D} + N\Omega J_{\text{H}} . \quad (21)$$

They further satisfy the Smarr-like mass formula [13],

$$M = \frac{D-2}{D-3} \frac{\kappa A_{\text{H}}}{8\pi G_D} + \frac{D-2}{D-3} N\Omega J + \Phi_{\text{H}} Q + \frac{D-5}{D-3} \tilde{\lambda} I , \quad (22)$$

where  $I$  denotes the integral

$$I = -\frac{1}{4\pi G_D} \int_{\Sigma} dS_{\sigma} \chi^{\nu} F_{\nu\rho} J^{\rho\sigma} , \quad (23)$$

and  $J^{\rho\sigma}$  is defined by

$$J^{\rho\sigma} = -\epsilon^{\rho\sigma\mu_1\mu_2\mu_3\dots\mu_{D-3}\mu_{D-2}} A_{\mu_1} F_{\mu_2\mu_3} \dots F_{\mu_{D-3}\mu_{D-2}} . \quad (24)$$

### 3.4 Scaling symmetry

The system of ODEs is invariant under the scaling transformation

$$r_{\text{H}} \rightarrow \gamma r_{\text{H}} , \quad \Omega \rightarrow \Omega/\gamma , \quad \tilde{\lambda} \rightarrow \gamma^{N-2} \tilde{\lambda} , \quad Q \rightarrow \gamma^{D-3} Q , \quad a_{\varphi} \rightarrow \gamma a_{\varphi} , \quad (25)$$

with  $\gamma > 0$ . We note that in two cases the scaling transformation does not change the CS coupling constant, namely, in the case  $\tilde{\lambda} = 0$  for arbitrary dimension  $D$  (i.e., in pure EM theory), and in the case  $D = 5$  for arbitrary  $\tilde{\lambda}$ . This is in accordance with the mass formula, Eq. (22). In both cases, the mass formula reduces to the standard Smarr formula, since the last term vanishes. Indeed, this is not accidental, but both features rely on the fact that the CS coupling constant is dimensionless only for  $D = 5$ , unless it vanishes [13].

## 4 Numerical Results

Apart from the case  $D = 5$ ,  $\tilde{\lambda} = \tilde{\lambda}_{\text{SG}} = 1/(2\sqrt{3})$  [11, 12], no charged rotating EMCS black hole solutions with spherical horizon topology are known analytically. Here we address the problem of finding such solutions numerically, and discuss their properties.

### 4.1 Numerical procedure

Owing to the existence of the first integral of the system of ODE's

$$\frac{r^{D-2} m^{N-2}}{f^{N-1}} \sqrt{\frac{mn}{f}} \left( \frac{da_0}{dr} + \frac{\omega}{r} \frac{da_{\varphi}}{dr} \right) - \tilde{\lambda} \hat{\varepsilon}_D 2^{D-2} (N-1)! a_{\varphi}^N = -\frac{4\pi G_D}{A(S^{D-2})} Q , \quad (26)$$

we eliminate  $a_0$  from the equations, replacing it in terms of the electric charge. This leaves a system of one first order equation (for  $n$ ) and four second order equations (for  $f$ ,  $m$ ,  $\omega$ , and  $a_{\varphi}$ ). In Eq. (26),  $\hat{\varepsilon}_D$  is just a sign, depending on the dimension  $D$ , and given by the expression

$$\hat{\varepsilon}_D \equiv (-1)^{N(N+1)/2} = (-1)^{(D^2-1)/8} . \quad (27)$$

For the numerical calculations we then introduce the compactified radial coordinate  $\bar{r} = 1 - r_{\text{H}}/r$  [17], and we take units such that  $G_D = 1$ . We employ a collocation method for boundary-value ordinary differential equations, equipped with an adaptive mesh selection procedure [18]. Typical mesh sizes include  $10^3 - 10^4$  points. The solutions have a relative accuracy of  $10^{-8}$ . The set of numerical parameters to be fixed for a particular solution is  $\{r_{\text{H}}, \Omega, Q, \tilde{\lambda}\}$ . By varying these parameters we generate families of EMCS black holes.

The scaling symmetry Eq. (25) leads us to consider  $D = 5$  black holes and black holes in  $D > 5$  dimensions separately. Since odd-dimensional EM black holes were investigated previously [10], we here concentrate on  $\tilde{\lambda} \neq 0$ .

Moreover, since the action Eq. (1) is invariant under the transformation

$$\{\tilde{\lambda}, Q\} \rightarrow \{(-1)^{N-1}\tilde{\lambda}, -Q\}, \quad (28)$$

it is sufficient to consider just two of the four possible sign combinations of  $\{\tilde{\lambda}, Q\}$ .

## 4.2 $D = 5$ EMCS black holes

For convenience we redefine the CS coupling constant,

$$\lambda = 2\sqrt{3} \tilde{\lambda}, \quad (29)$$

for  $D = 5$ . Additionally, owing to Eq. (28), without loss of generality we may choose  $\lambda \geq 0$ .

$D = 5$  EMCS black holes have been considered before for CS coupling  $\lambda_{\text{SG}}$  [11, 12, 13, 14] and for general coupling [15]. To briefly recall some of their main features, we exhibit in Fig. 1a the domain of existence of these black holes. Here the scaled angular momentum  $|J|/M^{3/2}$  of extremal EMCS black holes is shown versus the scaled charge  $Q/M$ <sup>1</sup> for four values of  $\lambda$ : the pure EM value  $\lambda_{\text{EM}} = 0$ , the supergravity value  $\lambda_{\text{SG}} = 1$ , the second critical value  $\lambda_{\text{cr}} = 2$ , and a value beyond this critical value,  $\lambda = 3$ . For a given value of  $\lambda$ , black holes exist only in the regions bounded by the  $J = 0$ -axis and by the respective curves. For fixed finite  $\lambda$ , there is an explicit asymmetry between solutions with positive and negative electric charge. The properties of EMCS black holes with positive  $Q$  are similar to those of EM black holes [10], whereas for EMCS black holes with negative  $Q$  surprising features are present.

The figure also shows stationary black holes with non-rotating horizon, i.e., black holes with horizon angular velocity  $\Omega = 0$  but finite total angular momentum. Such solutions are present only for  $\lambda \geq 1$ . For  $\lambda = 1$  they are extremal solutions, and form the vertical part of the  $Q < 0$  borderline of the domain of existence. For  $\lambda > 1$ , however, they are (with the exception of endpoints) non-extremal black holes, located in the interior of the respective domains of existence. In fact, the  $\Omega = 0$  lines divide these domains into two parts. The right part contains ordinary black holes, where the horizon rotates in the same sense as the angular momentum, while the left part contains black holes with unusual properties. When  $1 < \lambda < 2$ , all black holes in this region are counterrotating, i.e., their horizon rotates in the opposite sense to the angular momentum [15]. When  $\lambda > 2$ , further intriguing features appear.

---

<sup>1</sup>The scaling symmetry affects the physical quantities as follows,  $M \rightarrow \gamma^{D-3}M$ ,  $J \rightarrow \gamma^{D-2}J$ ,  $\mu_{\text{mag}} \rightarrow \gamma^{D-2}\mu_{\text{mag}}$ ,  $g \rightarrow g$ ,  $\kappa \rightarrow \kappa/\gamma$ , etc.



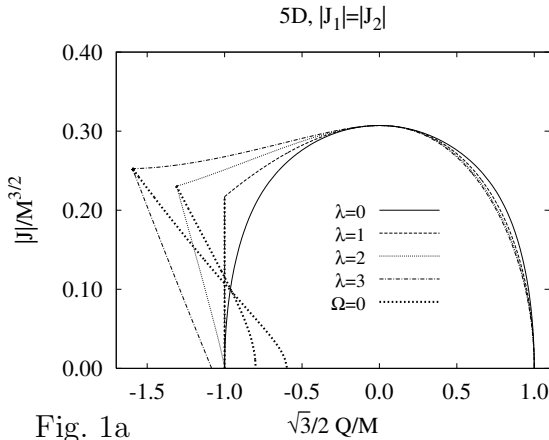


Fig. 1a

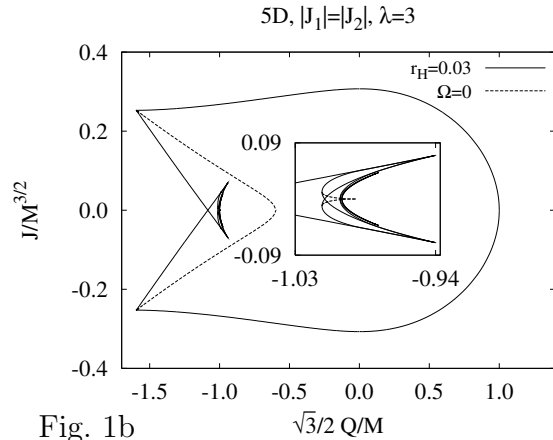


Fig. 1b

**Fig. 1** Scaled angular momentum  $J/M^{3/2}$  versus scaled charge  $Q/M$  for 5D EMCS black holes. a) Extremal and  $\Omega = 0$  solutions with CS coefficients  $\lambda = 0, 1, 2, 3$ . b) Almost extremal and  $\Omega = 0$  solutions with CS coefficient  $\lambda = 3$ .

As long as  $1 < \lambda < 2$  only static  $J = 0$  solutions exist, and consequently, the static extremal black holes are located on the borderline of the domain of existence. (Recall that static black holes are independent of  $\lambda$ .) However, beyond  $\lambda = 2$ , a continuous set of rotating  $J = 0$  solutions appears [15], whose existence relies on a special partition of the total angular momentum  $J$ , where the horizon angular momentum  $J_H$  is equal and opposite to the angular momentum  $J_\Sigma$  in the Maxwell field outside the horizon<sup>2</sup>. The static extremal black holes then no longer mark the lower left border of the domain of existence, which is now formed by extremal rotating  $J = 0$  black holes, as seen in Fig. 1a.

Moreover, beyond  $\lambda = 2$  the set of extremal solutions not only forms the boundary of the domain of existence, but continues well within this domain, until a static extremal black hole is reached in a complicated pattern of bifurcating branches. Insight into this set is gained in Fig. 1b, where (almost) extremal solutions are exhibited for CS coefficient  $\lambda = 3$ , together with non-static  $\Omega = 0$  solutions. Note, that all this new structure arises well within the counterrotating region, in the vicinity of the static extremal black holes.

To explore the properties of  $\lambda > 2$  EMCS black holes further, let us now consider non-extremal black holes. We exhibit in Fig. 2 a set of solutions for  $\lambda = 3$ , possessing constant charge  $Q = -10$  and constant (isotropic) horizon radius  $r_H = 0.1$ . Fig. 2a and 2b show the total angular momentum  $J$  and the horizon angular momentum  $J_H$ , respectively, as functions of the horizon angular velocity  $\Omega$ , Fig. 2c and 2d show the

<sup>2</sup>The numerical data indicate, that at  $\lambda = 2$  a continuous set of extremal rotating  $J = 0$  black holes with constant mass is present [15].

corresponding masses  $M$  and  $M_{\text{H}}$ , and Fig. 2e and 2f the gyromagnetic ratio  $g$  and the horizon area  $A_{\text{H}}$ .

Fig. 2a exhibits the four types of rotating black holes, as classified by their total angular momentum  $J$  and horizon angular velocity  $\Omega$ : Type I black holes correspond to the corotating regime, i.e.,  $\Omega J \geq 0$ , and  $\Omega = 0$  if and only if  $J = 0$  (static). Type II black holes possess a static horizon ( $\Omega = 0$ ), although their total angular momentum does not vanish ( $J \neq 0$ ). Type III black holes are characterized by counterrotation, i.e., the horizon angular velocity and the total angular momentum have opposite signs,  $\Omega J < 0$ . Type IV black holes, finally, possess a rotating horizon ( $\Omega \neq 0$ ) but vanishing total angular momentum ( $J = 0$ ).

As seen in Fig. 2b, the horizon angular momentum  $J_{\text{H}}$  of these black holes need not have the same sign as the total angular momentum  $J$ , and neither does the ‘bulk’ angular momentum  $J_{\Sigma}$ . In fact, as the horizon of the black hole is set into rotation, angular momentum is stored in the Maxwell field both behind and outside the horizon, yielding a rich variety of configurations. Starting from the static solution, a corotating branch evolves, along which  $J_{\text{H}}$  and  $J_{\Sigma}$  have opposite signs. After the first bifurcation  $\Omega$  moves back towards zero and so does  $J$ , but both  $J_{\text{H}}$  and  $J_{\Sigma}$  remain finite, retaining part of their built up angular momentum and thus their memory of the path, like in a hysteresis. This is important, since when moving  $\Omega$  continuously back to and beyond zero, the total angular momentum follows and changes sign as well. The horizon angular momentum, however, retains its sign. Thus the product  $\Omega J_{\text{H}}$  turns negative and remains negative up to the next bifurcation and still further, until  $\Omega$  reaches zero again.

The observation, that solutions with  $\Omega J_{\text{H}} < 0$  can be present, is crucial to explain the occurrence of black holes with negative horizon mass,  $M_{\text{H}} < 0$ , exhibited in Fig. 2d. The correlation between  $\Omega J_{\text{H}} < 0$  and  $M_{\text{H}} < 0$  black holes is evident here. In fact, the sets of  $\Omega J_{\text{H}} < 0$  and  $M_{\text{H}} < 0$  black holes almost coincide, when  $\kappa A_{\text{H}}$  is small, as seen from the horizon mass formula Eq. (21). The angular momentum stored in the Maxwell field behind the horizon is thus responsible for the negative horizon mass of the black holes. The total mass is always positive, however, as seen in Fig. 2c.

The correlation between  $\Omega J_{\text{H}} < 0$  and  $M_{\text{H}} < 0$  is further demonstrated in Fig. 3, where we exhibit  $J_{\text{H}}$  and  $M_{\text{H}}$  for black holes with smaller as well as larger (isotropic) horizon radii  $r_{\text{H}}$ . Whereas for larger values of  $r_{\text{H}}$  the set of negative horizon mass black holes decreases, it increases for smaller values of  $r_{\text{H}}$ . In fact, as  $r_{\text{H}}$  decreases, more branches of solutions appear in the vicinity of the static solution, giving rise to more branches of negative horizon mass black holes.

Another interesting feature of these charged rotating EMCS black holes is their gyromagnetic ratio  $g$ , exhibited in Fig. 2e. The gyromagnetic ratio is unbounded, reaching any real value including zero. The main consequence of this is that, contrary to pure EM theory, a vanishing total angular momentum does not readily imply a vanishing magnetic moment and viceversa.

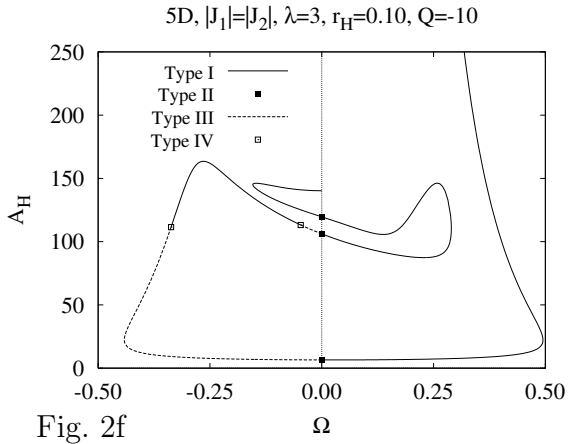
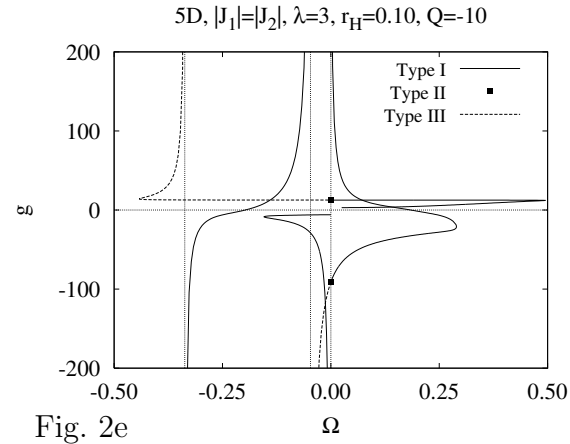
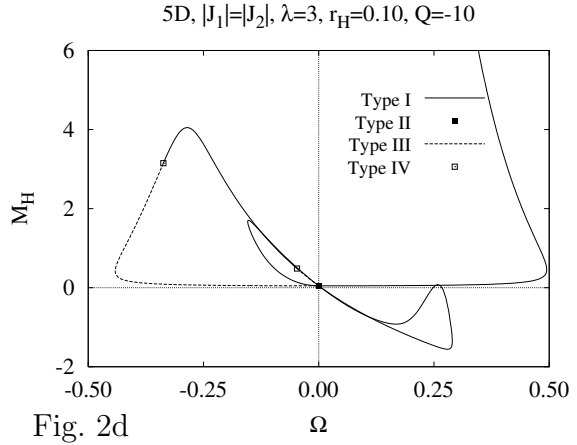
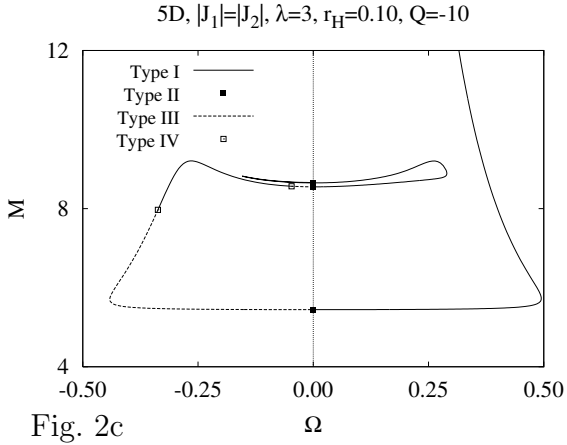
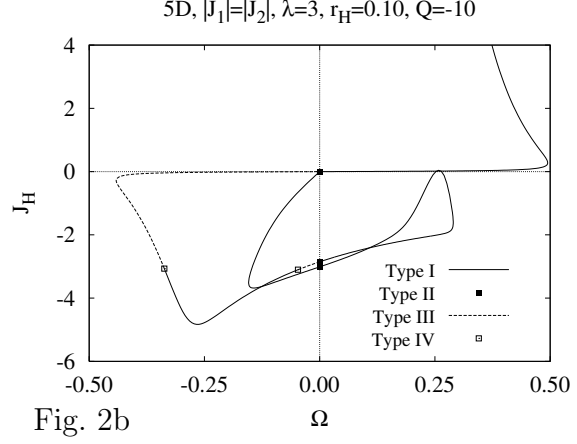
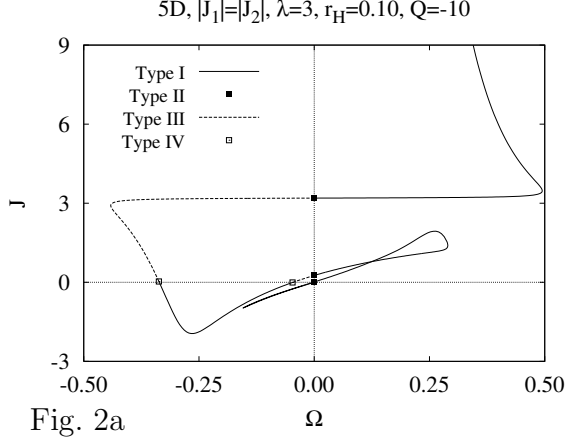


**Fig. 2** Properties of 5D non-extremal  $\lambda = 3$  EMCS black holes with charge  $Q = -10$  and horizon radius  $r_H = 0.1$ . a) angular momentum  $J$ , b) horizon angular momentum  $J_H$ , c) mass  $M$ , d) horizon mass  $M_H$ , e) gyromagnetic ratio  $g$ , f) horizon area  $A_H$  versus horizon angular velocity  $\Omega$ .

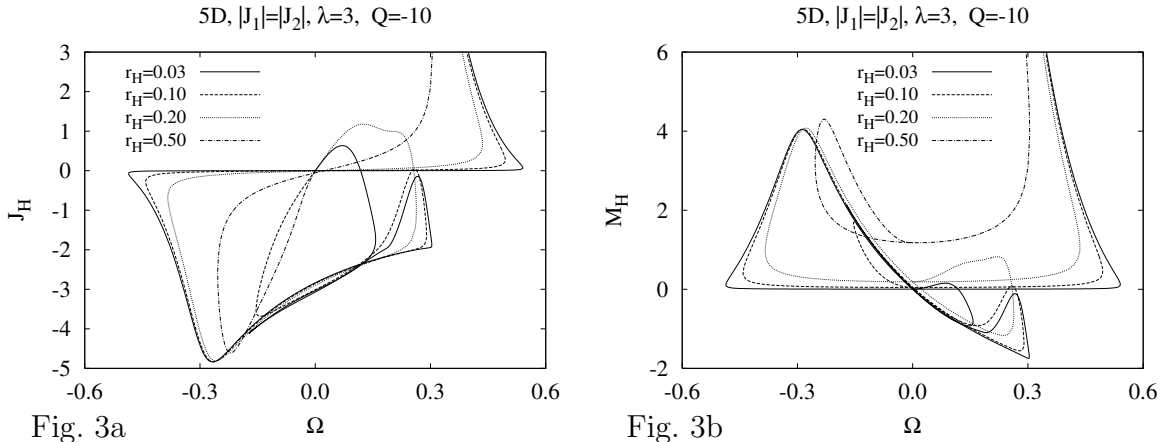


**Fig. 3** Properties of 5D non-extremal  $\lambda = 3$  EMCS black holes with charge  $Q = -10$  and horizon radii  $r_H = 0.03, 0.1, 0.2$  and  $0.5$ . a) horizon angular momentum  $J_H$ , b) horizon mass  $M_H$  versus horizon angular velocity  $\Omega$ .

### 4.3 $D > 5$ EMCS black holes

Unlike in  $D = 5$ , the CS coupling constant is dimensionful when  $D > 5$ , and consequently changes under scaling transformations Eq. (25), unless  $\tilde{\lambda} = 0$ . Thus any feature present for a certain non-vanishing value of  $\tilde{\lambda}$  will be present for any other non-vanishing value, when the charge is scaled correspondingly. To classify the critical behaviour of the solutions we therefore consider classes of solutions labelled by the scale invariant ratio  $\lambda_Q$ ,

$$\lambda_Q = \tilde{\lambda}/|Q|^{(D-5)/2(D-3)}. \quad (30)$$

Otherwise, black holes of  $D > 5$  EMCS theories exhibit very similar properties to  $D = 5$  EMCS black holes. Besides regions containing black holes with features resembling those of EM black holes, there are regions where black holes reside, possessing all those new features. Assuming  $Q < 0$ , the sign of  $\tilde{\lambda}$  associated with the appearance of these new types of black holes coincides with  $-\hat{\varepsilon}_D$  (while for  $Q > 0$  one needs to employ Eq. (28)).

We exhibit in Fig. 4a sets of extremal 7D solutions, choosing the same value of the charge in all sets, while varying  $\tilde{\lambda}$ . In 7D, the first critical value is  $\lambda_Q = -0.0414$ . Here the first  $\Omega = 0$  solution appears. Counterrotating black holes then exist only for values of the ratio  $\lambda_Q$  above this critical value. The second critical value characterizes the limit above which non-static  $J = 0$  solutions are present, and where solutions are no longer uniquely specified by their global charges. In 7D this value is  $\lambda_Q = -0.2101$ . We note, that the sets of  $\Omega = 0$  solutions, also exhibited in the figure, always connect extremal solutions, whose mass assumes an extremal value as well, in accordance with

the first law. At the second critical value of  $\lambda_Q$ , the lower endpoint of the  $\Omega = 0$  set of solutions precisely reaches a static extremal black hole.

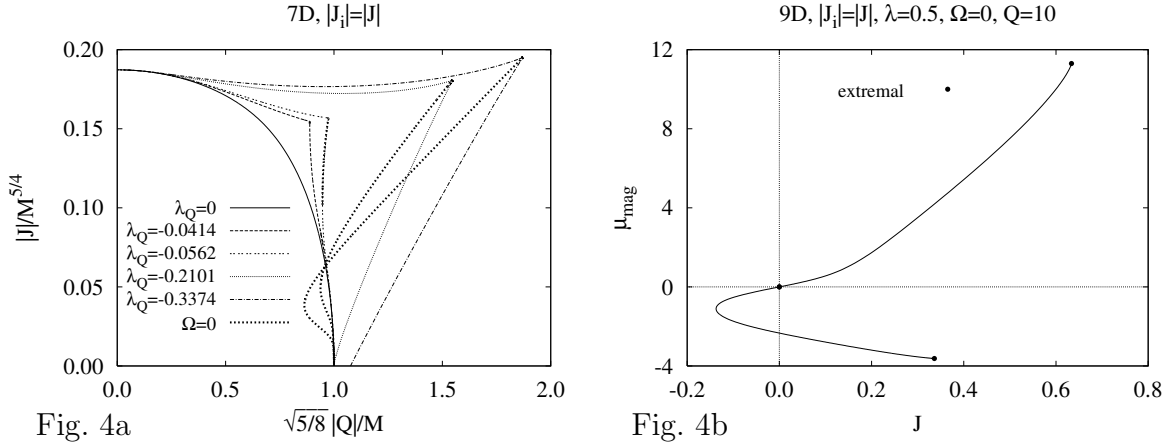


**Fig. 4** a) Scaled angular momentum  $J/M^{5/4}$  versus scaled charge  $Q/M$  for (almost) extremal 7D EMCS black holes and  $\Omega = 0$  solutions for  $\lambda_Q = 0, -0.0414, -0.0562, -0.2101, -0.3374$  and charge  $Q = 10$ . b) Magnetic moment  $\mu_{\text{mag}}$  versus total angular momentum  $J$  for 9D EMCS black holes with  $\Omega = 0$  for  $\tilde{\lambda} = 0.5$  and charge  $Q = 10$ .

In Fig. 5 we demonstrate that the four types of rotating black holes, as classified by their total angular momentum  $J$  and horizon angular velocity  $\Omega$ , are also present for  $D > 5$ . Interestingly, in  $D = 9$ , beside I. corotating black holes, II. non-static  $\Omega = 0$  black holes, III. counterrotating black holes, IV. non-static  $J = 0$  black holes, a further type of black holes appears: V. non-static  $\Omega = J = 0$  black holes. This is seen in Fig. 4b, where the magnetic moment is exhibited for a set of 9D  $\Omega = 0$  black holes. Clearly, there appears a non-static  $\Omega = J = 0$  solution with finite magnetic moment. We further illustrate in Fig. 5 that these EMCS black holes are no longer uniquely characterized by their global charges, i.e., the uniqueness conjecture does not hold in general for  $D \geq 5$  EMCS stationary black holes with horizons of spherical topology<sup>3</sup>.

We illustrate in Fig. 6 that  $D > 5$  EMCS black holes can also possess negative horizon mass  $M_H$ , by exhibiting sets of  $D = 7$  and  $D = 9$  black holes. As in  $D = 5$  dimensions, the angular momentum stored in the Maxwell field behind the horizon is responsible for this phenomenon. Finally, the gyromagnetic ratio  $g$  is unbounded as well for  $D > 5$  EMCS black holes, reducing the correlation between angular momentum and magnetic moment.

<sup>3</sup>Previous counterexamples involved black rings [16].

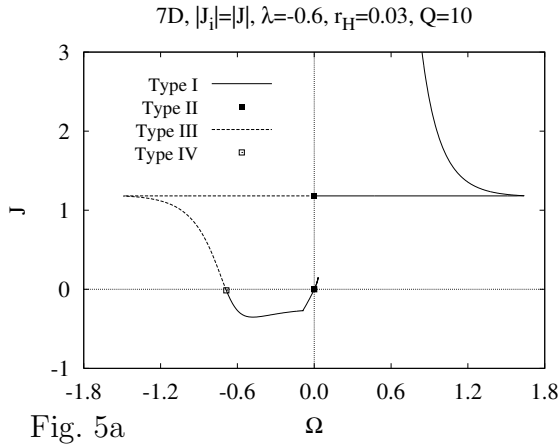


Fig. 5a

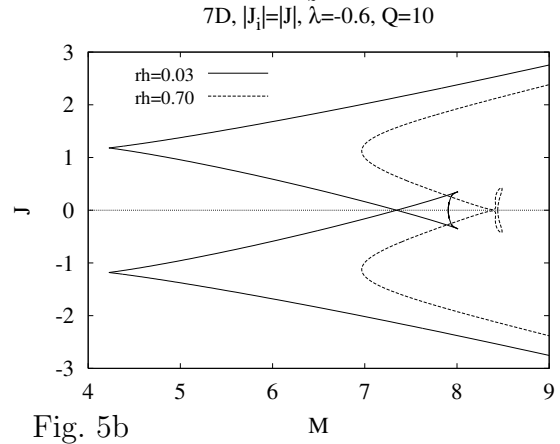


Fig. 5b

**Fig. 5** Angular momentum  $J$  of 7D non-extremal  $\tilde{\lambda} = -0.6$  EMCS black holes with charge  $Q = 10$  a) versus horizon angular velocity  $\Omega$  for horizon radius  $r_H = 0.03$ , b) versus mass  $M$  for horizon radii  $r_H = 0.03, 0.7$ .

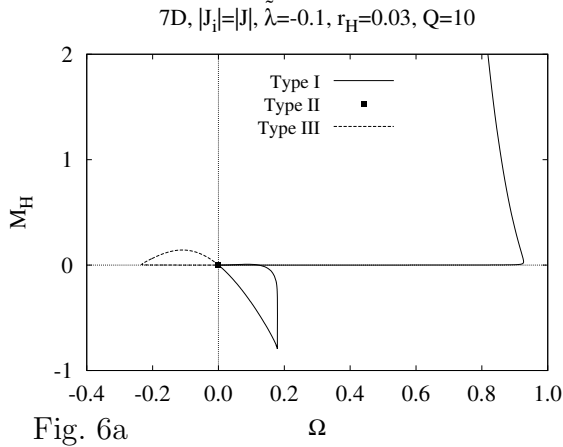


Fig. 6a

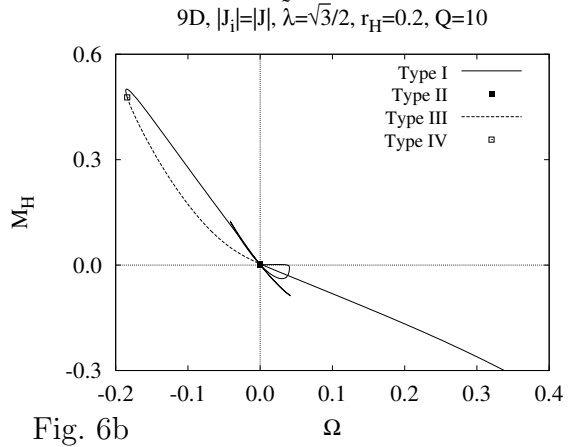


Fig. 6b

**Fig. 6** Horizon mass  $M_H$  of non-extremal EMCS black holes with charge  $Q = 10$  versus horizon angular velocity  $\Omega$  a) for 7D, horizon radius  $r_H = 0.03$ ,  $\tilde{\lambda} = -0.1$ , b) for 9D, horizon radius  $r_H = 0.2$ ,  $\tilde{\lambda} = \sqrt{3}/2$ .

## 5 Conclusions

We have considered charged rotating black holes of EMCS theory in odd dimensions, which are asymptotically flat and possess a regular horizon of spherical topology. When all their angular momenta have equal-magnitude, a system of 5 ordinary differential equations results [10], which we have solved numerically.

EMCS black holes exhibit remarkable features, not present for EM black holes. Classifying the EMCS black holes by their total angular momentum  $J$  and horizon angular velocity  $\Omega$ , we find several types of black holes: I. corotating black holes, i.e.,  $\Omega J \geq 0$ , II. black holes with static horizon and non-vanishing total angular momentum, i.e.,  $\Omega = 0$ ,  $J \neq 0$ , III. counterrotating black holes, where the horizon angular velocity and the total angular momentum have opposite signs, i.e.,  $\Omega J < 0$ , and IV. black holes with rotating horizon and vanishing total angular momentum, i.e.,  $\Omega \neq 0$ ,  $J = 0$ . Furthermore, in  $9D$  type V. black holes appear: non-static black holes with static horizon and vanishing total angular momentum, i.e.,  $\Omega = J = 0$ .

As the horizon of static EMCS black holes is set into rotation, angular momentum is stored in the Maxwell field both behind and outside the horizon. Following paths through configuration space, the horizon angular momentum  $J_H$  and the ‘bulk’ angular momentum  $J_\Sigma$  can retain part of the angular momentum built up in the Maxwell field, even when the horizon angular velocity vanishes again. Thus they retain the memory of the path, like a hysteresis. Consequently, solutions with  $\Omega J_H < 0$  appear, which possess a negative horizon mass,  $M_H < 0$ , as long as  $\kappa A_H$  is sufficiently small. The angular momentum stored in the Maxwell field behind the horizon is therefore responsible for the negative horizon mass of these black holes. Their total mass is always positive, however <sup>4</sup>.

Moreover, EMCS black holes are no longer uniquely characterized by their global charges, i.e., the uniqueness conjecture does not hold in general for  $D \geq 5$  EMCS stationary black holes with horizons of spherical topology, and the gyromagnetic ratio of these black holes may take any real value, including zero.

### Acknowledgement

FNL gratefully acknowledges Ministerio de Educación y Ciencia for support under grant EX2005-0078.

## References

- [1] R. P. Kerr, Phys. Rev. Lett. **11** (1963) 237;  
E. T. Newman, E. Couch, K. Chinnapared, A. Exton, A. Prakash, R. Torrence, J. Math. Phys. **6** (1965) 918.
- [2] V. Frolov, A.Zelnikov, and U. Bleyer, Ann. Phys. (Leipzig) **44** (1987) 371;  
D. Rasheed, Nucl.Phys. **B454** (1995) 379;  
J.H. Horne and G.T. Horowitz, Phys. Rev. **D46** (1992) 1340.
- [3] B. Kleihaus, J. Kunz, and F. Navarro-Lérida, Phys. Rev. **D69** (2004) 081501.

---

<sup>4</sup>The occurrence of a negative horizon mass has been also reported recently in the context of  $4D$  black holes surrounded by perfect fluid rings [19].

- [4] W. Israel, *Commun. Math. Phys.* **8** (1968) 245;  
D. C. Robinson, *Phys. Rev. Lett.* **34** (1975) 905;  
P. Mazur, *J. Phys.* **A15** (1982) 3173;  
M. Heusler, *Black Hole Uniqueness Theorems*, (Cambridge University Press, 1996).
- [5] M. S. Volkov and D. V. Galt'sov, *Sov. J. Nucl. Phys.* **51** (1990) 747;  
P. Bizon, *Phys. Rev. Lett.* **64** (1990) 2844;  
H. P. Künzle and A. K. M. Masoud-ul-Alam, *J. Math. Phys.* **31** (1990) 928.
- [6] B. Kleihaus and J. Kunz, *Phys. Rev. Lett.* **79** (1997) 1595; *Phys. Rev.* **D57** (1998) 6138.
- [7] R. C. Myers, M. J. Perry, *Ann. Phys. (N.Y.)* **172** (1986) 304.
- [8] see e.g. D. Youm, *Phys. Rept.* **316** (1999) 1.
- [9] J. Kunz, F. Navarro-Lérida, and A. K. Petersen, *Phys. Lett.* **B614** (2005) 104.
- [10] J. Kunz, F. Navarro-Lérida, J. Viebahn, *Phys. Lett.* **B 639** (2006) 362.
- [11] J. C. Breckenridge, D. A. Lowe, R. C. Myers, A. W. Peet, A. Strominger, C. Vafa, *Phys. Lett.* **B381** (1996) 423;  
J. C. Breckenridge, R. C. Myers, A. W. Peet, C. Vafa, *Phys. Lett.* **B391** (1997) 93.
- [12] M. Cvetič, H. Lü, C. N. Pope, *Phys. Lett.* **B598** (2004) 273; *Phys. Rev.* **D70** (2004) 081502; Z.-W. Chong, M. Cvetič, H. Lü, C. N. Pope, *Phys. Rev. Lett.* **95** (2005) 161301.
- [13] J. P. Gauntlett, R. C. Myers, P. K. Townsend, *Class. Quantum Grav.* **16** (1999) 1.
- [14] C. A. R. Herdeiro, *Nucl. Phys.* **B582** (2000) 363;  
P. K. Townsend, *Annales Henri Poincare* **4** (2003) 183.
- [15] J. Kunz, F. Navarro-Lérida, *Phys. Rev. Lett.* **96** (2006) 081101.
- [16] R. Emparan, H. S. Reall, *Phys. Rev. Lett.* **88** (2002) 101101;  
H. Elvang, *Phys. Rev.* **D68** (2003) 124016;  
H. Elvang, R. Emparan, *J. High Energy Phys.* **0311** (2003) 035;  
R. Emparan, *J. High Energy Phys.* **0403** (2004) 064;  
S. S. Yazadjiev, *Phys. Rev.* **D73** (2006) 104007.



- [17] B. Kleihaus, J. Kunz, Phys. Rev. Lett. **86** (2001) 3704;  
B. Kleihaus, J. Kunz, F. Navarro-Lérida, Phys. Rev. **D66** (2002) 104001; Phys. Rev. Lett. **90** (2003) 171101; Phys. Rev. **D69** (2004) 064028; Phys. Lett. **B599** (2004) 294; Phys. Rev. **D69** (2004) 081501(**R**).
- [18] U. Ascher, J. Christiansen, R. D. Russell, Mathematics of Computation **33** (1979) 659; ACM Transactions **7** (1981) 209.
- [19] M. Ansorg, D. Petroff, gr-qc/0607091.